Technical Report

Simulation Technology for Titanium Oxide Layer Interference Color

Noriko NAGATA*
Kensuke TOBITANI
Mitsuhito KAMEI
Toshio AKAGI
Kazuhiro TAKAHASHI
Sakuya YAMAMURA

Abstract

The titanium oxide layer undergoes diverse color changes due to thin film interference. Because of its high designability, expectations for various applications are increasing. Accurate representation of the interference color and texture of the oxide layer formation in simulation will lead to design support. In this study, we investigated the simulation of interference colors of a thin oxide layer on titanium in two steps. The first is a half vector-based thin film interference model for expressing the interference color macroscopically, and the second is a microfacet-based thin film interference model for expressing the surface roughness structure microscopically. Both simulation results show that an average color difference of within 5.0 and Grade 4 in the color tolerance classification, which are sufficient for practical use.

1. Introduction

The demand for high designability materials is increasing in manufacturing. Titanium creates various interference colors depending on the thickness of the oxide film formed by anodization (hereinafter referred to as anodized oxide film). Also, various textures are produced by the surface unevenness of anodized titanium. The superimposition of these various interference colors and surface unevenness creates rich designability. Interference colored titanium is being deployed in various fields such as buildings (**Fig. 1**) and ornaments. Accurate representation of titanium designability by CG simulation is expected to facilitate the visualization of the desired design and to support the design process.

Material texture expression technology by CG simulation is used in various fields such as product design and online marketing. Particularly, the importance of texture representation is increasing in the fields related to the creation of values such as design and attractiveness. To accurately express the color and texture of a material, a physically based modeling and rendering approach that focuses on the physical phenomena peculiar to the material is effective in simulating the optical phenomena of the material.

We conducted a two-step study on the simulation of interference colors using an anodized oxide film. The first step is a model (half vector-based thin film interference model) that macroscopically explains the optical phenomenon characteristic of the anodized oxide film through which an interference color is visible in the diffuse reflection direction and a simulation that is applied to SD titanium samples (with a cold rolled surface and relatively small unevenness).[1] The second step is a model that microscopically explains the roughness structure of the titanium surface (microfacet-based thin film interference model) and a simulation that is applied to ND titanium samples (with a dull surface and relatively large unevenness).[2] The simulation results confirmed that the titanium samples have practically satisfactory color accuracy with an average color difference (ΔE) of within 5.0 and Grade 4 in the color tolerance classification. The two models and the simulation results are described below.

Fig. 1 View of color-decorated building using titanium oxide layers (Hotel Marques de Riscal)

* Dr. (Eng.), Professor, School of Engineering, Kwansei Gakuin University / Director, Kwansei Gakuin Institute of Kansei Value Creation
2-1 Gakuen, Sanda City, Hyogo Pref. 669-1337

2. Simulation by Half Vector-based Thin Film Interference Model

2.1 Characteristics of thin film interference by anodized oxide film

The thin film interference caused by the anodized oxide film is characteristic in that interference colors are observed not only in the specular reflection direction, but also in the diffuse reflection direction. Figure 1 shows the appearance of a building decorated with anodized titanium sheets. Despite the complicated shape, clear interference colors are observed over wide areas. This means that the interference colors are widely distributed in the diffuse reflection direction as well. **Figure 2** shows a principle model conventionally used to explain the thin film interference. With this model, the interference color is observed only in the specular reflection direction. In other words, this model cannot explain the thin film interference caused by the anodized oxide film.

2.2 Characterization of interference colors and surface roughness using titanium samples

The anodization voltage is changed to change the anodized oxide film thickness and to produce various interference colors as shown in **Fig. 3**. We first measured the interference colors by measuring the omnidirectional spectral reflectance of titanium samples, measured the surface roughness of the titanium samples with a surface roughness measuring instrument, and microscopically observed the local interference colors assumed from the surface roughness measurements. The upper left blue sample 2 in Fig. 3 was used as the sample.

2.2.1 Measurement of interference colors

To check the interference colors on the anodic oxide surfaces in the diffuse reflection direction, the spectral reflectance was measured with a Digital Fashion spectral bidirectional reflectance distribution function (sBRDF) measuring device. This measuring device consists of a spectrometer, a light source, and a sample stand and can measure the sBRDFs. The optical system of the sBRDF measuring device is shown in **Fig. 4**.

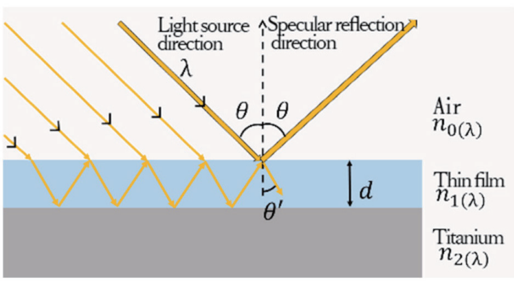

Fig. 2 Principle model of thin layer interference

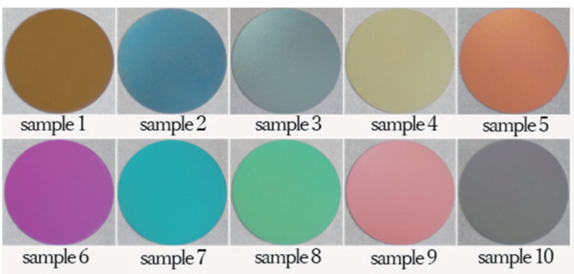

Fig. 3 View of various titanium plates with oxide layer (SD)

The sBRDF measuring device changes the light source direction (θ_l, φ_l) and viewing direction (θ_v, φ_v) with respect to the sample and measures the spectral reflectance. **Figure 5** shows the angular distribution of the interference colors obtained by measuring the sBRDFs of the blue sample and converting it to RGB.

In Fig. 5, a highlight is observed in the specular reflection direction region where the light quantity is large. As the angle in the diffuse reflection direction increases, a bright blue color similar to that when the sample is visually perceived is confirmed. When the angle in the diffuse reflection direction becomes larger, the color changes from dark blue to navy blue due to the decrease in the light quantity. When the light quantity from the light source is reduced with a neutral density (ND) filter, a bright blue color is confirmed even in the specular reflection direction of the highlight region.

These results confirmed that a color similar to the interference color visually perceived in the specular reflection direction is recognized on the anodized oxide film surface even in the diffuse reflection direction.

2.2.2 Measurement of surface roughness

Next, the roughness of the titanium surface is evaluated. This is necessary for modeling the structural color due to thin film interference by rough surface scattering. It has been confirmed that the macro roughness curve of the titanium surface is almost the same as the roughness curve of the anodized oxide film surface. (This applies when the anodization voltage is about several tens of volts. The anodization voltage of the blue sample is 25 V and satisfies this anodization voltage condition.) That is, it shows that the macroscopic thickness distribution of the anodized oxide film can be assumed to be almost uniform. Therefore, in this paper, the titanium surface roughness is evaluated by measuring surface roughness of the anodized oxide film. **Figure 6** shows the measurement results of the surface roughness curve of sample 2 measured with a contact type roughness measuring instrument. The arithmetic average roughness

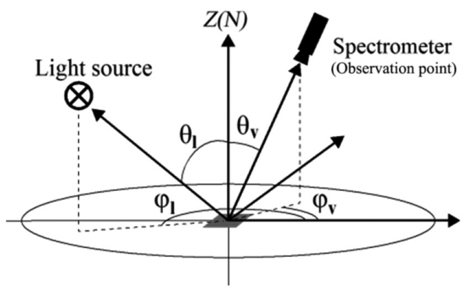

Fig. 4 Optical system of sBRDF measuring equipment

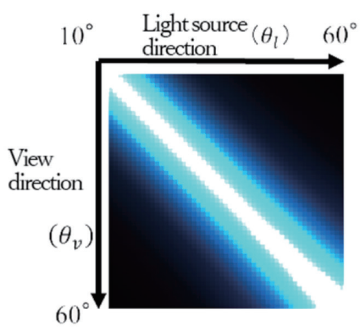

Fig. 5 Measured interference color distribution of blue color plate (sample 2)

Ra was 268.0 nm, and the maximum height roughness *Rmax* was 1 821.0 nm.

The evaluation of the optical smoothness of the sample surface is discussed by using the Rayleigh criterion of Equation (1).

$$h = \lambda/8 \cos\theta \tag{1}$$

where λ is the wavelength and θ is the incident angle. If the surface roughness is smaller than h, the surface is optically "smooth". If it is greater than h, the surface is optically classified as "rough". Using Equation (1) by assuming that the wavelength range visible to the human eye is approximately 380 to 780 nm, h is 47.5 to 195.0 nm when the incident angle is changed in the range of 0 to 60°. The *Ra* value of the blue sample used in our study was 268.0 nm and much larger than the h value. That is, the anodized oxide film surface of the sample is optically rough. The titanium surface whose film thickness is substantially uniform is also considered to be a rough surface.

2.2.3 Observation of local interference colors

The interference color on the sample surface was checked from microscopic images. The results are shown in **Fig. 7**.

Figure 7 (a) shows a microscope image under the specular reflection conditions of a light source direction (zenith angle) of 0° and a viewing direction (zenith angle) of 0°. By reducing the illumination light quantity, the same blue interference color as in Fig. 3 is observed. Figure 7 (b) shows a microscope image under the diffuse reflection conditions of a light source direction of 45° and a viewing direction of 0°. The color ranges from dark blue to close to black as a whole. When the illumination light quantity was increased as shown in Fig. 7 (c) under the conditions shown in Fig. 7 (b), a blue interference color of the same hue as shown in Fig. 7 (a) increases locally, so that the same interference as in the specular reflection direction also holds in the diffuse reflection direction. According to the above study results, we propose a model for showing the interference color in the diffuse reflection direction on an optically rough anodized titanium surface.

2.3 Half vector-based thin film interference model

The half vector means a direction between the light source direction and the viewing direction and is a concept widely used in the CG field. Generally, it is used to express the intensity distribution of reflection light in the specular reflection components in a physically correct way. It can also express the wavelength distribution of reflection light if the wavelength of light is taken into consideration.

The half vector-based thin film interference model is schematically illustrated in **Fig. 8**. The figure shows the observation from the viewing direction θ_v, which is different from the specular reflection direction, with respect to the light source direction θ_l. On the rough surface, the existence of microfacets with various directions can be assumed. Focusing on an aggregation of only those microfacets that have as normal lines half vectors in the light source direction and the viewing direction, the specular reflection conditions locally hold and thin film interference occurs. This model can explain the thin film interference color in the diffuse reflection direction.

2.4 Simulation method

Based on the proposed thin film interference model, the spectral reflectance of the reflection light is obtained by simulation.

In Fig. 8, θ_l and θ_v are the angles of the light source direction and the viewing direction, respectively, d is the thickness of the anodized oxide film, λ is the wavelength of the incident light, and $n_{0(\lambda)}$, $n_{1(\lambda)}$, and $n_{2(\lambda)}$ are the complex refractive index at the wavelength λ of the air layer, the anodized oxide film, and the titanium layer, respectively. Using these parameters, the spectral reflectance of the reflection light is calculated from Snell's law and Fresnel's equations.

First, the reflectance in the conventional principle model (Fig. 2) is calculated by Equation (2).

$$R = \left| \frac{r_{12} + r_{23} e^{i\delta}}{1 + r_{23} r_{12} e^{i\delta}} \right|^2 \tag{2}$$

where r_{12} and r_{23} are the Fresnel reflectance coefficients. Also, δ is the phase difference and is given by

$$\delta = 4\pi n_{1(\lambda)} d \cos\theta' / \lambda \tag{3}$$

where θ' is the refraction angle and is calculated by Equation (4) using the incident angle θ according to Snell's law.

$$\theta' = \sin^{-1}(n_{0(\lambda)} \sin\theta / n_{1(\lambda)}) \tag{4}$$

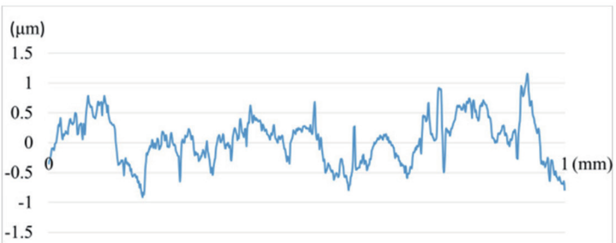

Fig. 6 Surface roughness curve of oxide layer on blue color plate (sample 2)

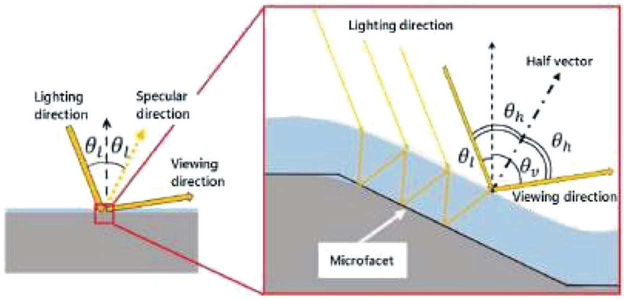

Fig. 8 Model of layer interference based on half vector

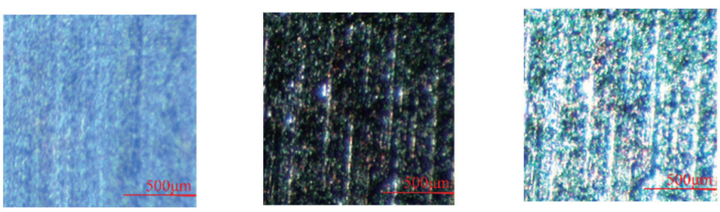

(a) Light 0°, View 0°

(b) Light 45°, View 0°

(c) Image with increased average brightness of (b)

Fig. 7 Microscopic images of blue color plate

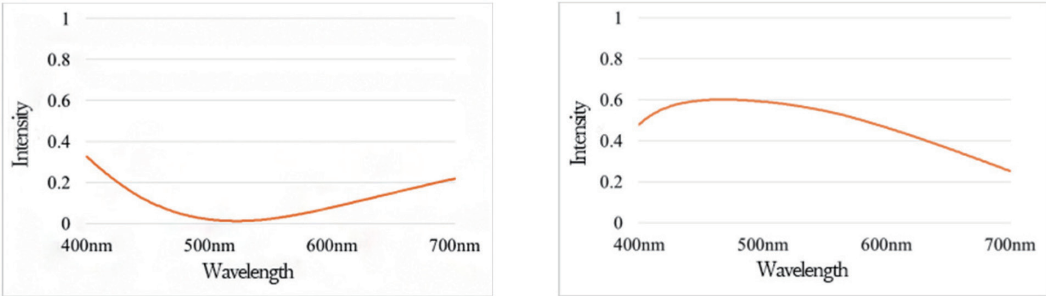

(a) Film thickness 30 nm (b) Film thickness 70 nm

Fig. 9 Results of simulation (light: 10°, camera: 45°)

Table 1 Estimated thickness of oxide layer of 10 samples

Sample number	1	2	3	4	5	6	7	8	9	10
Estimated thickness (nm)	15.9	50.8	60.6	87.5	121.4	138.4	160.6	173.9	226.6	264.4

Table 2 Color difference of 10 samples

Sample number	1	2	3	4	5	6	7	8	9	10
Color difference	2.9	3.2	2.5	4.3	7.3	5.6	4.1	4.9	9.9	5.4

Our half vector-based thin film interference model regards the interface between the anodized oxide film and the titanium layer as a set of microfacets and shows the thin film interference on the microfacets where the specular reflection conditions hold in the light source direction and the viewing direction. So, instead of the light source direction θ in Equation (4) of the principle model of thin film interference, θ_h in Equation (5) is substituted as the incident angle.

$$\theta_h = (\theta_l + \theta_v)/2 \qquad (5)$$

Thin film interference broadly occurs in the diffuse direction but it also occurs locally by specular reflection. As a result, the interference color can be observed. This phenomenon can be represented by a model.

Figure 9 shows the results of simulation by the model. The spectral reflectance was determined for two film thicknesses d of 30 nm and 70 nm as examples. Public information was used for the values of the real part and the imaginary part of the complex refractive index $n_{1(\lambda)}$ of the anodized oxide film. To deal with diffuse reflection, we also considered multiple reflections of low intensity in the calculation of spectral reflectance.

The spectral reflectance in the diffuse reflection direction could be calculated by applying the half vector-based thin film interference model. The model showed the wavelength dependence of the spectral reflectance of titanium from the wavelength dependence of the complex refractive index of the anodized oxide film and titanium. It also showed the change in the spectral reflectance with the change in the film thickness of the anodized oxide film.

2.5 Simulation results and evaluation

The color difference is obtained from the spectral reflectance calculated by the simulation and from the measured spectral reflectance. The obtained color difference is then evaluated.

To obtain the spectral reflectance, the thickness of the anodized oxide film is required as a simulation parameter. The anodization voltage of the sample is known but its anodized oxide film thickness is not. Therefore, it is necessary to estimate the film thickness. In this study, the spectral reflectance is obtained by changing the film thickness parameter. The film thickness at which the mean square error from the measured spectral reflectance is minimal is calculated and used as the estimated film thickness. The estimated film thickness is shown in **Table 1**.

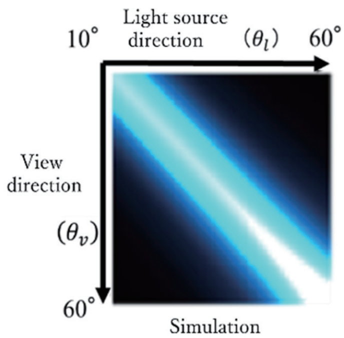

Fig. 10 Simulated interference color distribution of blue color plate

Next, simulations of the spectral reflectance were performed from the estimated film thickness by using Equations (2) to (5) and by changing the light source direction and the viewing direction. **Figure 10** shows the angular distribution of the interference colors calculated from the simulated spectral reflectance. The figure confirmed that the calculated angular distribution of the interference colors is close to that measured.

In addition, the color differences from the measured values were calculated. Since this study targets the interference colors in the diffuse reflection direction, the average color differences of the samples were calculated by excluding the specular reflection region. The results are given in **Table 2**. The average color difference of all ten samples was 5.0. This is Grade 4 in the color tolerance classification and is sufficiently accurate for practical use. The error factors may be the behavior of light not expressed by the thin film interference model and the errors peculiar to the sBRDF measuring device.

2.6 CG representation

The samples were represented by CG using the model. The samples were rendered by setting the type of light source (a D65 light source), shooting environment (light source position, shooting target position, camera position, shooting space size), and camera parameters (focal length, sensor size, aperture, shutter speed, etc.) the same as when shooting actual images. A camera shot image and a CG image are comparatively shown in **Fig. 11**. The CG image shows a bluish hue similar to that of the camera shot image in the overall diffuse reflection direction. It accurately represents the change in the color hue with the change from the specular reflection direction to the diffuse reflection direction.

3. Microfacet-based Thin Film Interference Model

3.1 Microfacet theory

The half vector-based thin film interference model described in the previous section is a macro approximate model that focuses on the interference colors peculiar to titanium and produced in the diffuse reflection direction. The model is effective when the surface unevenness is relatively small like in the SD titanium samples and when the appearance probability of microfacet normal directions (microfacet normals distribution) can be assumed to be constant. To represent titanium with more complicated surface unevenness like the ND samples, a model that appropriately expresses the microfacet normals distribution is required.

In the CG field, the representation of light reflections from uneven surfaces has been investigated as microfacet theory or normals distribution function (NDF) research. The microfacets are a concept (assuming their set). There were no studies that actually visualized the microfacets as images.

3.2 Visualization of microfacet structure by optical microscopy

An attempt was made to observe titanium samples with an optical microscope to obtain a model of the microfacet normal distribution on the titanium sample surface. As a result, we succeeded in observing the titanium surface property or optical phenomenon (hereinafter referred to as microfacet structure) corresponding to the microfacet theory.

The target sample is shown in **Fig. 12**. After rolling, large unevenness was transferred by roll dull finishing onto the surface of the titanium sample. Finally, the titanium sample was anodized at 82.5 V (this sample is hereinafter referred to as the ND sample). The surface of the ND sample has a macro structure produced by roll dull finishing. It has also been confirmed that a several micron order microstructure that the titanium surface originally had remains in the convex portions.[3] The above results suggest that the surface shape model addresses a complex rough surface with both a macrostructure and a microstructure as shown in **Fig. 13**. ND samples that have not been anodized (hereinafter referred to as bare samples) were also observed for comparison.

A KEYENCE VHX-900F digital microscope was used as the optical microscope. As the observation conditions, standard white light was used as the incident light, the angle was 0° for both the light source direction and the viewing direction, the lens was an apochromat lens, and the magnification was X1 000. The size of the region observed with the optical microscope is 347.8 μm × 260.9 μm on the surface of the ND sample.

The obtained images are shown in **Fig. 14**. From Fig. 14(a), it

Fig. 12 View of titanium plate with oxide layer (ND)

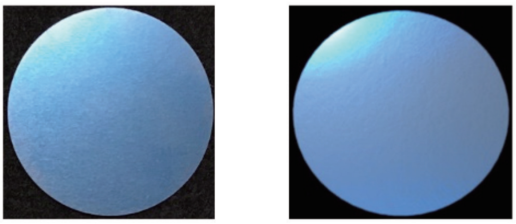

(a) Real image (b) CG image

Fig. 11 Real image and CG image of titanium

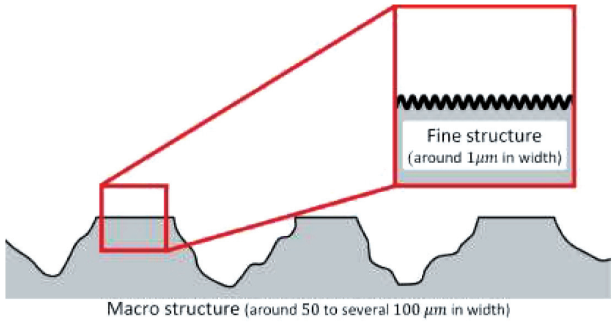

Fig. 13 Surface-shape model of ND sample

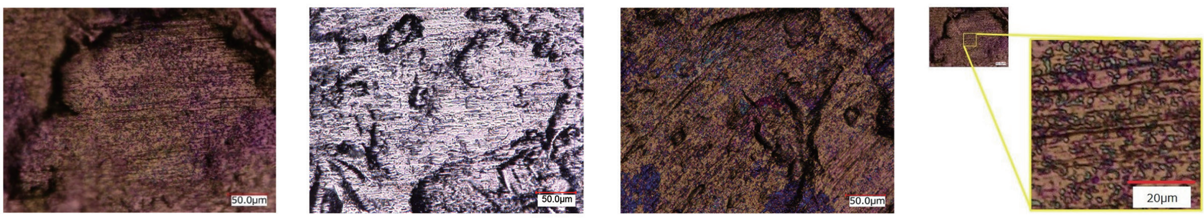

(a) ND sample (b) Bare sample (c) Bare sample with oxide layer (d) Locally enlarged image of (a)

Fig. 14 Microscope images

can be confirmed that various colors are scattered in a grainy pattern. Figure 14 (b) shows a bare sample observed under the same optical conditions. Unlike in the ND sample, no grainy color development can be confirmed. The bare sample was anodized and observed as shown in Fig. 14 (c). The same grainy color development as observed again with the ND sample was confirmed with the anodized bare sample. From this result, it was confirmed that the grainy color development originated from the anodized oxide film.

3.3 Microfacet-based thin film interference model

3.3.1 Proposal of model

The phenomenon in which we can observe grainy color development simply with anodized oxide film samples is proposed as the microfacet-based thin film interference model shown in **Fig. 15**. Figure 15 (a) shows an ND sample with a thin film formed on the titanium surface by anodization. The phase difference in thin film interference differs with the difference in the normal direction of the microfacet and produces different colors on the anodized oxide film surface. When the titanium surface has no anodized oxide film, on the other hand, the light incident on the titanium surface reflects in various directions due to the difference in the microfacet normal direction as shown in Fig. 15 (b) and does not produce different colors. The color grains observed in Fig. 14 are about 1 to 3 μm in diameter. These were considered to be images in which the microfacet structure is visualized by the model of Fig. 15. Since it was confirmed that innumerable microfacets are scattered over the entire area of the same sample, it was also confirmed that the microfacet structure became apparent regardless of the region to be observed. There are studies that have observed the structure of about 10 μm crystal grains in commercially pure titanium with a microscope, but no investigations have captured microstructures in the order of a few micrometers. From the above results, it was considered that the “microfacet structure” was visualized for the first time by the optical microscope observation of anodized titanium.

3.3.2 Verification of microfacet structure by height map

To check whether the grainy color development originates from the microfacet structure, the surface shape of the grainy color development was reconstructed three dimensionally from the height map.

The height map was measured by moving the sample stand of the optical microscope in the height direction, collecting the movement amounts and image data, and determining the focus position in pixel units by image processing. **Figure 16** shows a microscope image and a height map to which the position information obtained here is tied. The range of the read height map was 0.000 to 17.600 μm over the entire image.

Next, several points were randomly extracted from Fig. 16 (a) as grainy color development points. Each surface shape was three-dimensionally reconstructed from the measured height map. **Figure 17** shows the results of the reconstruction (only two points here).

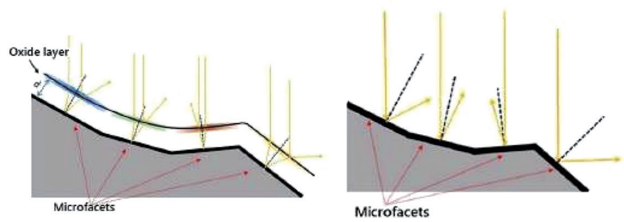

(a) ND sample (b) Bare sample

Fig. 15 Model of thin-film interference based on microsurface normal

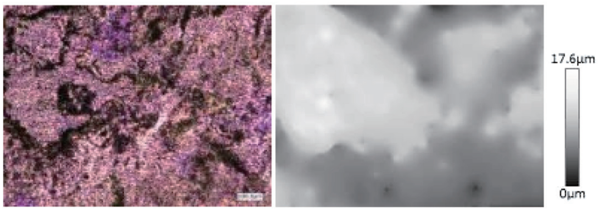

(a) Microscope image (b) Height map

Fig. 16 Microscope image and height map with matching location information

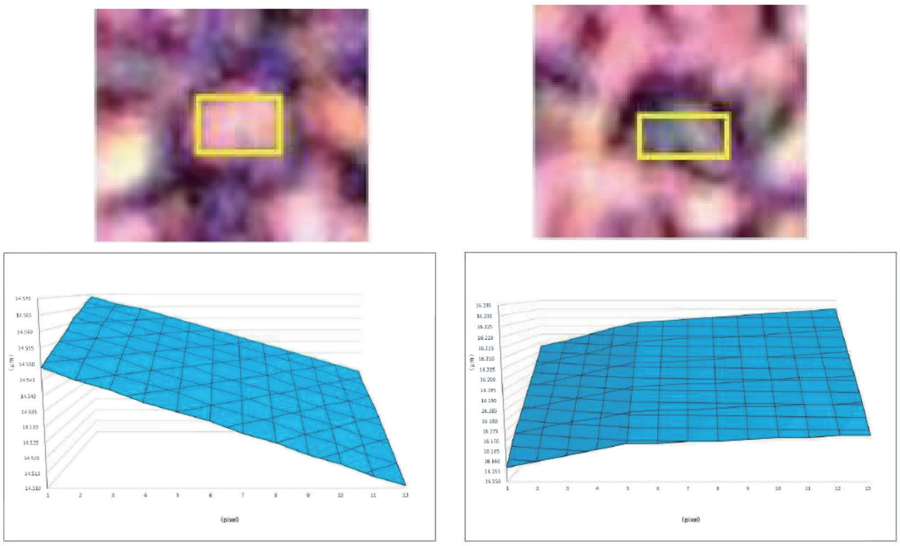

(a) 1-color example (b) 2-color example

Fig. 17 Microscope images and surface shapes reproduction results by height map; Vertical axis is height, and horizontal axis is pixels.

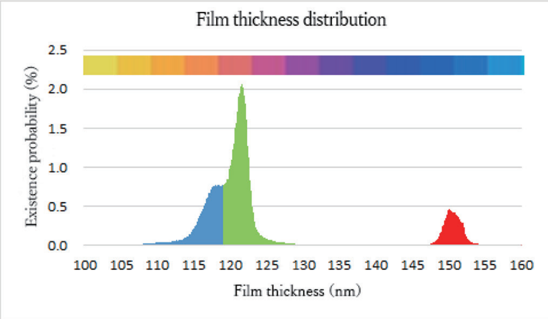

(a) Three Gaussian distributions in film thickness distribution

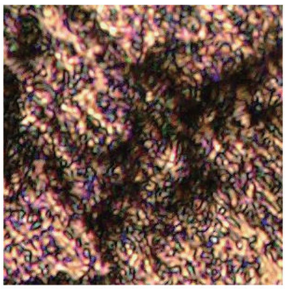

(b) Microfacet image

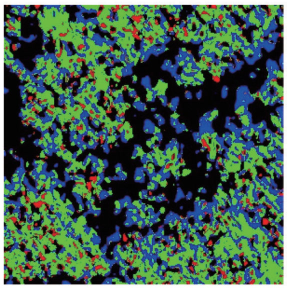

(c) Visualization of microfacet image

Fig. 18 Film thickness distribution and microfacet images

From the figure, it can be seen that the convex and concave portions of the surface are a few nanometers or two orders of magnitude smaller than the wavelength of light and that the surface shape is composed of convex and concave portions not large enough to affect the interference phenomenon. That is, the sample in Fig. 17(a) is almost flat, and the sample in Fig. 17(b) can be regarded as being composed of two flat surfaces similar to the flat surface in Fig. 17(a). When observing the relationship between the colors of the grainy development points and the surface shape, it was found that one color in the microscope image corresponds to one flat surface in Fig. 17(a) and that the microscope image consists of two colors with respect to two flat surfaces in Fig. 17(b).

From this, it was confirmed that the grainy color development and the flat surfaces correspond to each other and concluded that these flat surfaces are the microfacets in the microfacet normal-based thin film interference model. Also, if the film thickness is assumed to be constant within the field of view of the microscope, we consider that the color development changes under the influence of the microfacet slope.

From the above, it can be assumed that the localization of the grainy color development is due to the microfacet structure. It is suggested that the microfacet-based thin film interference model can calculate the microfacet normal distribution in a complex surface structure.

3.3.3 Calculation of microfacet normal distribution using microfacet images

From the optical microscope images (hereinafter referred to as microfacet images), the microfacet normal distribution is obtained by color image analysis. The microfacet normal distribution is calculated as described below.

(1) Calculation of normal map
The normal directions of the microfacets composed of the points of the height map (Fig. 16(b)) are calculated. A normal map in which the position information is tied to the microfacet image (Fig. 16(a)) is obtained.

(2) Estimation of film thickness
In the microfacet image, a region of interest (ROI) is set in the region where the film thickness can be assumed to be constant. (In this case, the region of interest is a square whose sides are 55.1 μm (255 pixels) wide.) Next, in the ROI, pixels whose saturation is smaller than a threshold (set to 15 in this case) are masked. This is to exclude the specular reflection regions and the shadow regions. From a simulation using the half vector-based thin film interference model, the Lab[*1] values determined from the normal directions when the film thickness is assumed are compared with the Lab values of the microfacet image. The film thickness at which the average color difference (ΔE) becomes minimum is determined.

(3) Estimation of normal directions
The normal direction and the Lab values are calculated from a simulation using the film thickness determined in (2). The normal direction at which the color difference (ΔE) from the Lab value of the image becomes minimum is obtained and taken as the normal direction of the pixel.

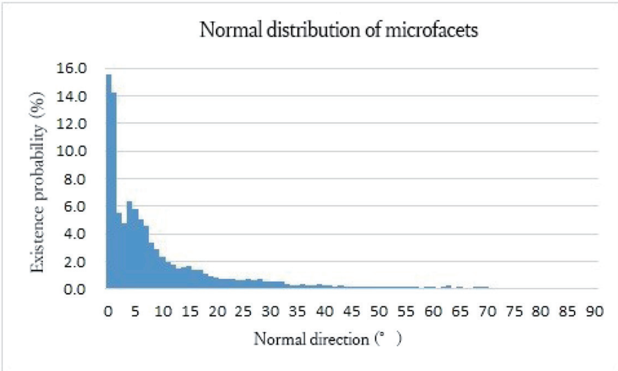

Fig. 19 Microfacets normal distribution

Figures 18 and **19** show the estimated film thickness distributions and the microfacet normal distributions in the entire regions calculated by the above procedure, respectively. The estimated film thickness was 100.0 to 160.0 nm. The average color difference of the pixels calculated was stable at about 5.0. This suggests that good estimation results were obtained. Both the film thickness distribution and the normals distribution are considered to be distributions in which some strain component is added to the typical Gaussian distribution.

The film thickness distribution (Fig. 18(a)) is interpreted as a composite of the three Gaussian distributions. Figure 18(c) shows a microfacet image visualized in three types of film thickness regions

*1 Defined by the Commission Internationale de l'Eclairage (CIE) and used as a color representation method throughout the world. L is lightness in values of 0 to 100, a is red/green in values of −100 to +100, and b is blue/yellow in values of −100 to +100. For example, L: 65, a: 57, and b: 70 indicate an orange color globally.

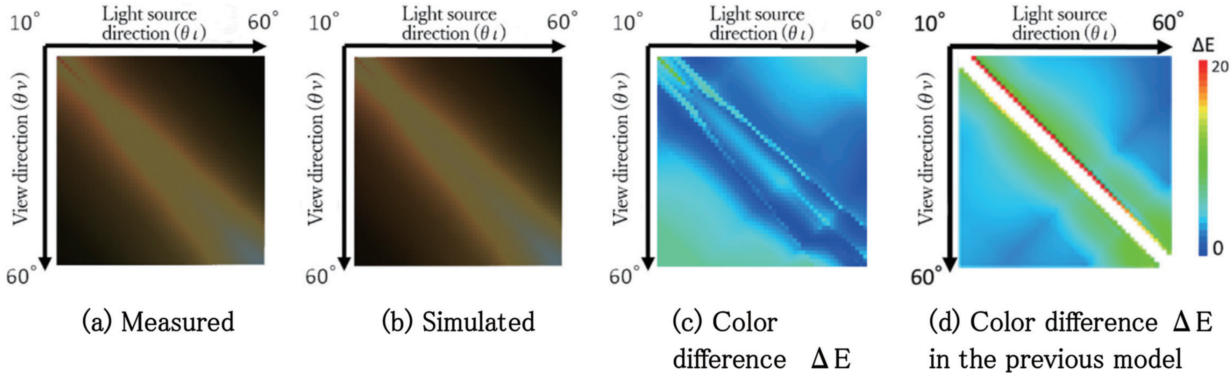

Fig. 20 Results of interference color distribution

(film thickness regions of 119 nm and below, 120 to 139, and 140 nm and above are shown as blue, green, and red, respectively). The regions that are significantly different in color (Fig. 18(b)) correspond to the regions where the film thickness is large (Fig. 18(c)). Also, the regions around the shadow regions (Fig. 18(b)) correspond to the regions where the film thickness is small (Fig. 18(c)). It is suggested that local thickness changes appear as a composite of three Gaussian thickness distributions.

The normals direction distribution of Fig. 19 is interpreted as a composite of a small-variance Gaussian distribution with a mode of 0° and a large-variance Gaussian direction distribution with a mode of 0°. When these are applied to the surface shape model shown in Fig. 13, it is hypothesized that the small-variance Gaussian direction distribution is due to the structure of the convex portions where the characteristics of the microstructure of the SD sample remain and that the large-variance Gaussian direction distribution is due to the macrostructure of the concave portions characteristic of the ND sample. Based on these hypotheses, we plan to model the normals distribution and to verify the factors that cause the film thickness to change locally.

3.4 Simulation method

The spectral reflectance of the reflection light is obtained by a simulation, based on the microfacet-based thin film interference model. In addition to the half vector-based calculation procedure described in Section 2.4, the microfacet normal distributions and film thickness distributions obtained in Section 3.3.3 are used as probability density functions.

$$R_{in,out} = \Sigma_{\theta_m} \Sigma_d \, r(\theta_{in}+\theta_m, d)\, g(d)\, f(\theta_m) \cos(\theta_{out}-\theta_m) \cos(\theta_{in}+\theta_m) \cos(\theta_{out}+\theta_{in}-2\theta_m)^n \quad (6)$$

where $R_{in,out}$ is the reflectance in the incoming direction *in* and in the outgoing direction *out*, $r(\theta,d)$ is the reflectance by the half vector-based thin film interference model in the normal direction θ and at the film thickness d, θ_{in}, θ_{out}, and θ_m are the incoming angle, outgoing angle, and microfacet normal angle, respectively, $f(\theta)$ is the probability density function of the normal direction θ, $g(d)$ is the probability density function of the film thickness d, and n is a parameter of the cosine lobe model.

The microfacet-based thin film interference model has made it possible to calculate the reflection intensity and to calculate the spectral reflectance of interference colors including both specular reflection light and diffuse reflection light.

3.5 Simulation results and evaluation

Figures 20(a) and 20(b) show the angular distribution of spectral reflectance calculated by a simulation and the measured angular distribution of spectral reflectance, respectively. When the two sets of results were compared, the average color difference ΔE was 4.98 as shown in Fig. 20(c). A color difference tolerance of Grade 4 was achieved as shown in Fig. 20(d). The previous half vector-based interference color model achieved an average color difference of 5.0 as shown in Fig. 20(d) but evaluated only the diffuse reflection light, excluding the specular reflection light. A significant improvement in accuracy and expressiveness was achieved in this model.

4. Conclusions

The physical modeling and simulation methods of various interference colors and surface unevenness conditions that support the designability of anodized titanium were investigated. A half vector-based thin film interference model for modeling interference colors and a microfacet-based thin film interference model for modeling surface unevenness conditions were proposed in this study. In the study process, we were able to visualize the microfacet structure for the first time and to estimate the film thickness distribution and the microfacet normal distribution. We ultimately achieved a highly accurate simulation with an average color difference of about 5.0.

In the future, we will identify the distortion factors included in the microfacet normal distribution, model the normal distribution function (NDF), and incorporate the effects of low-saturation regions such as optical highlight regions and shadow regions to establish a method for comprehensively simulating anodized titanium oxide films with complex surface structures.

References

1) Fujii, H., Tobitani, K., Tani, Y., Kamei, M., Nagata, N., Akagi, T., Takahashi, K., Yamamura, S.: Color of Oxide Layered Coating on Titanium Considering Interference from Fine Structure. IEICE Transactions on Information and Systems (Jpn.), D, J102-D (6), 464–472 (2019)
2) Fujimoto, S., Tobitani, K., Kamei, M., Nagata, N., Akagi, T., Takahashi, K., Yamamura, S.: Normal Distribution Model of Microfacets Based on Color Image Analysis for Titanium Surface with Thin Film Interference Color. Journal of the Japan Society for Precision Engineering (Jpn.). 86 (12), 1051–1056 (2020)
3) Akashi, T., Shiraishi, T., Ogawa, S., Matsuse, Y., Morihara, H.: Skin Pass Rolling Characteristic of Tin Plates with Dull Work Rolls —Numerical Analysis of Skin Pass Rolling of Tin Plate—. Shinnittetsu Sumikin Giho. (401), 35–49 (2015)


Noriko NAGATA
Dr. (Eng.)
Professor, School of Engineering,
Kwansei Gakuin University
Director,
Kwansei Gakuin Institute of Kansei Value Creation
2-1 Gakuen, Sanda City, Hyogo Pref. 669-1337


Kensuke TOBITANI
Dr. (Eng.)
Visiting Professor,
Kwansei Gakuin Institute of Kansei Value Creation
Associate professor,
Faculty of Information Systems,
University of Nagasaki


Mitsuhito KAMEI
Dr. (Eng.)
Visiting Professor,
Kwansei Gakuin Institute of Kansei Value Creation


Toshio AKAGI
General Manager, Head of Dept.
Production Management Research Dept.
Intelligent Algorithm Research Center
Process Research Laboratories


Kazuhiro TAKAHASHI
General Manager, Head of Dept., Dr. Eng.
Titanium & Stainless-steel Research Dept.
Materials Reliability Research Lab.
Steel Research Laboratories


Sakuya YAMAMURA
Researcher
Instrumentation & Processing Research Dept.
Instrumentation & Control Research Lab.
Process Research Laboratories